SUPPORTING INFORMATION

for

Suprathermal Magnetospheric Atomic and Molecular Heavy Ions

At and Near Earth, Jupiter, and Saturn: Observations and Identification

S.P. Christon[1], D.C. Hamilton[2], D.G. Mitchell[4], J.M.C. Plane[3], and S.R. Nylund[4]

[1] Focused Analysis and Research, Columbia, Maryland, USA
[2] University of Maryland, Department of Physics, College Park, Maryland, USA
[3] School of Chemistry, University of Leeds, Leeds, U.K.
[4] Johns Hopkins University Applied Physics Laboratory, Laurel, Maryland, USA

Contents of this file

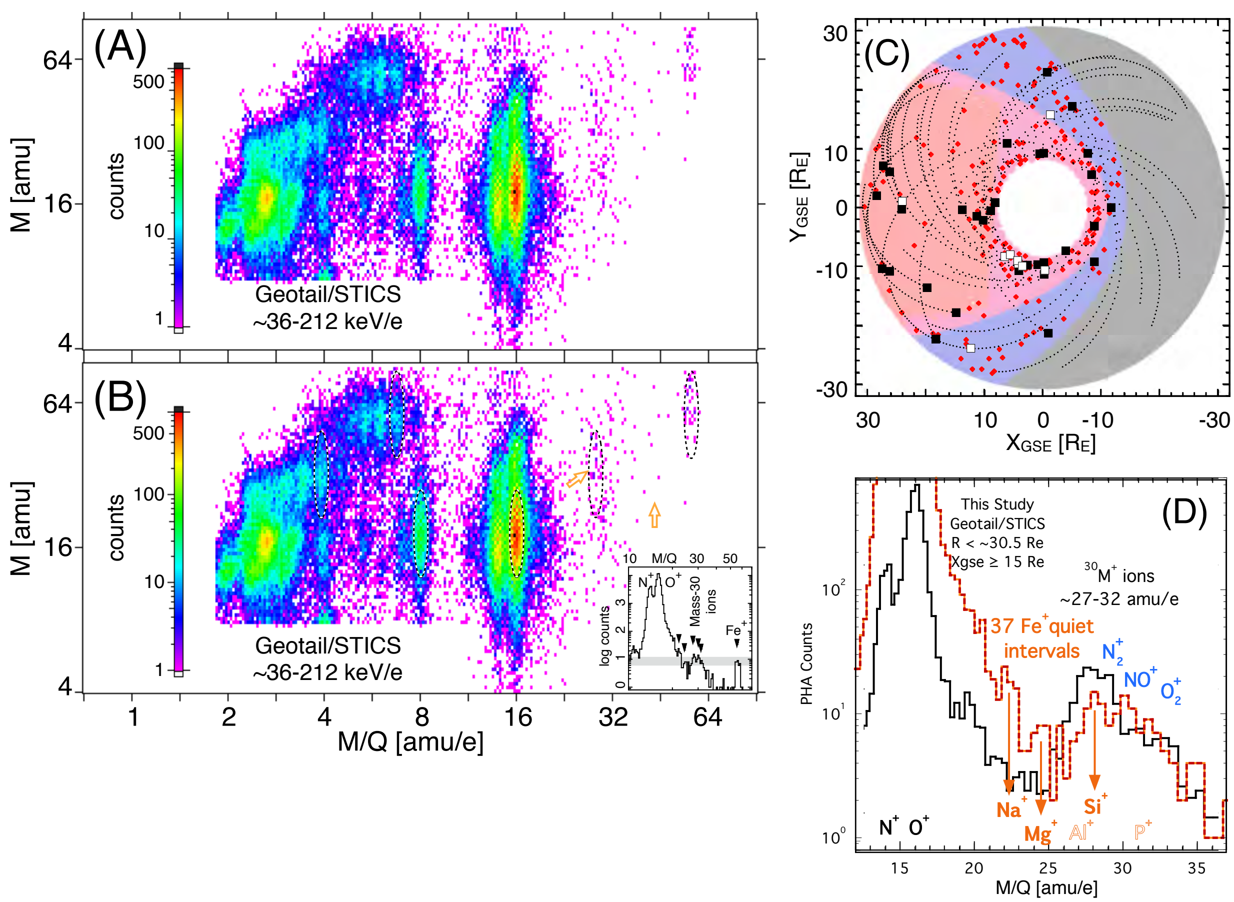

Figure S5. Data shown in panels A (unannotated) and B (annotated), are from intervals **spanning all plasma regimes** which terminate at Fe^+ measurements in the SPHERE or SHEATH. They were chosen at times of minimal $^{28}Mq^+$ presence by Christon et al. (2017). The $^{28}Mq^+$ M/Q range can include both ionospheric N_2^+ and Si^+, as well as lunar origin Si^+ and Fe^{+2}. Each of the 37 intervals is >25 hours long (~70% are ≥36 hr) and was selected to capture prior solar wind flows possibly carrying solar wind or lunar origin Fe^{+2} or Fe^+ that might result in the observed Fe^+ from these selected SPHERE and SHEATH intervals. Kp ranges from 0 to 6 (mean and mode near Kp ~ 3o) during these intervals. Dashed ovals in panel B show the similarity of atomic ion PHA distribution shapes for several readily identifiable ions including: ionospheric origin O^+, O^{+2}, and Fe^+, and solar wind origin Si^{+7} and Fe^{+8}. An oval is also drawn where Si^+ should be centered (noted by the upper gold arrow, compare to panel A). Si^+ is a major ionospheric origin ion (Plane et al., 2018) and one of the major lunar pickup ions (e.g., Mall et al., 1998; Figure 17 of Saito et al., 2010; Poppe et al., 2015). The PHA counts in the Fe^+ oval appear to be comparable to or greater than the counts in the Si^+ oval. No observational study has yet reported measuring lunar Fe^+ (e.g., Kirsch et al., 1998, using Wind/STICS, reported no observed Fe^+). The vertical open gold arrow at ~40-44 amu/e shows where lunar PUI Ca^+ and CO_2^+, often readily identified outside Earth's magnetosphere in our data (Figures 5A, 5B, and S3), are absent in these data. The panel-B-inset shows peaks (triangles) at Na^+, Mg^+, Al^+, Si^+, and possibly P^+ with peak and summed PHA counts comparable (gray band) to the Fe^+ peak as expected for ionospheric origin ions (e.g., Plane et al., 2018), but not for lunar pickup ions (e.g., Halekas et al., 2015). (C) Hourly points (small black dots) identify the orbit segments. Small red dots identify other Fe^+ measurement locations in the selected SPHERE and SHEATH regimes whose data are not included in panels A and B. Large squares identify these orbit's Fe^+ measurement locations; the 9 white (33 black) squares indicate Fe^+ PHAs measured when the Moon was (not) sunward of Earth (see the Figure 7 discussion). (D) PHA data at >10 amu/e from the panel-B-inset are compared to our far-upstream data from Figure 9.

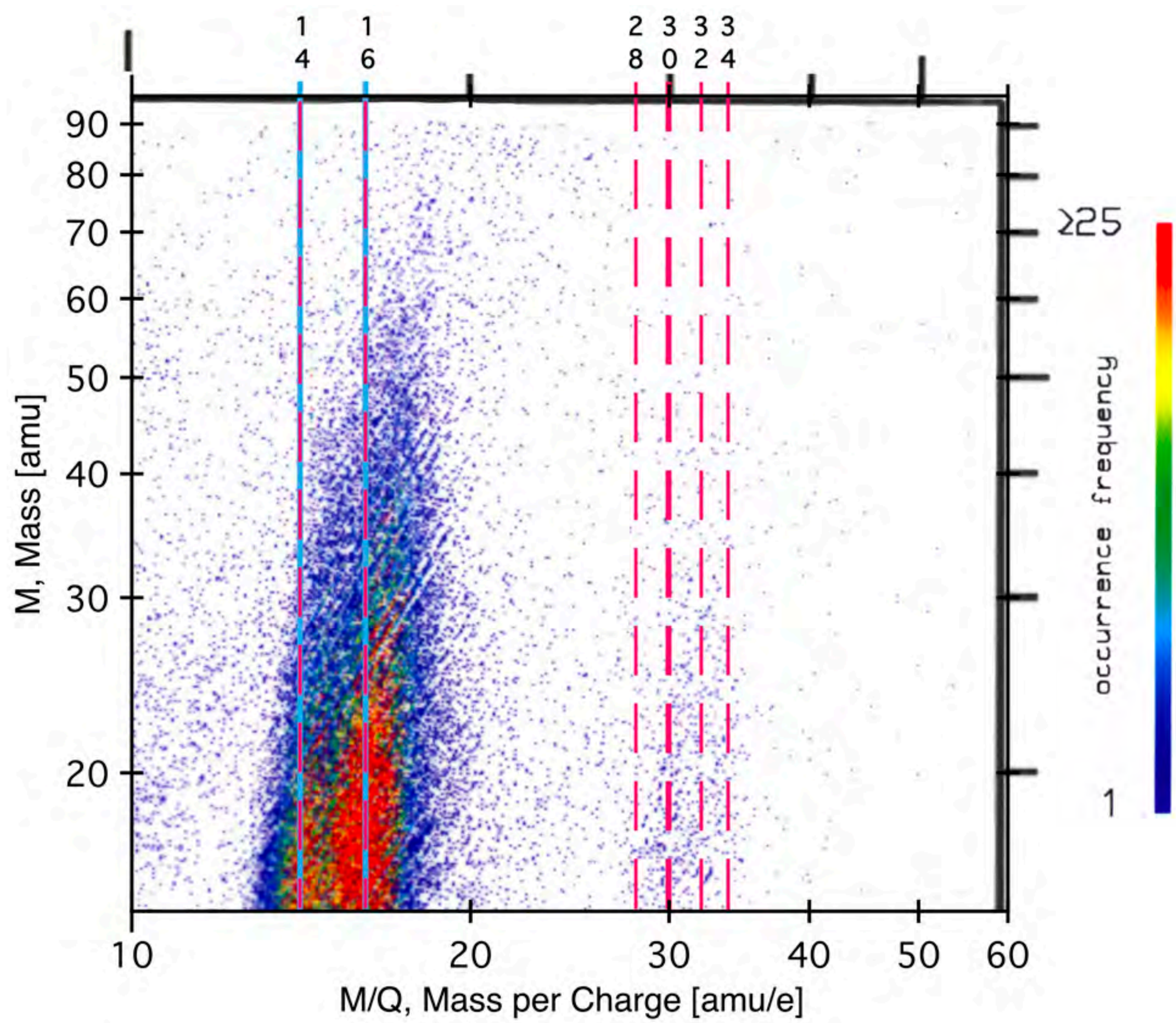

Figure S6. A section of Plate 1 from *Christon et al.* [1994a] containing N^+, O^+, and the molecular ions measured from ~7 to ~9 Re in Earth's quasi-trapping region by the Ampte/CCE/CHEM ion spectrometer from 1985-091 to 1985-211. CHEM had a M/Q response from ~0.7 to ~50 amu/e. Although molecular ions were not the focus of *Christon et al.* [1994a], they nominally identified the molecular ions broadly centered from ~28 to ~34 amu/e as NO^+ and O_2^+ following the identification by *Klecker et al.* [1986]. A set of plot axes and fiducials at 14, 16, 28, 30, 32, and 34 amu/e are drawn over the original figure. The N^+ and O^+ fiducials are fairly well-centered at 14 and 16 amu/e, respectively. When *Christon et al.* [2013] studied the CO^+ and O_2^+ ions at Saturn, we developed a fuller understanding of the molecular ion responses in the CHEM/ STICS/CHEMS type instruments in magnetospheric environs. Our current understanding of the molecular ion response, based on the description in *Christon et al.* [2013] (supplementary information Section B), is developed further herein (see text). Given this understanding, we feel that O_2^+, as well as the dominant N_2^+ and NO^+, might possibly contribute to these ~7-9 Re molecular ion measurements, although without recollecting and analyzing the Ampte data, this is merely a supposition.

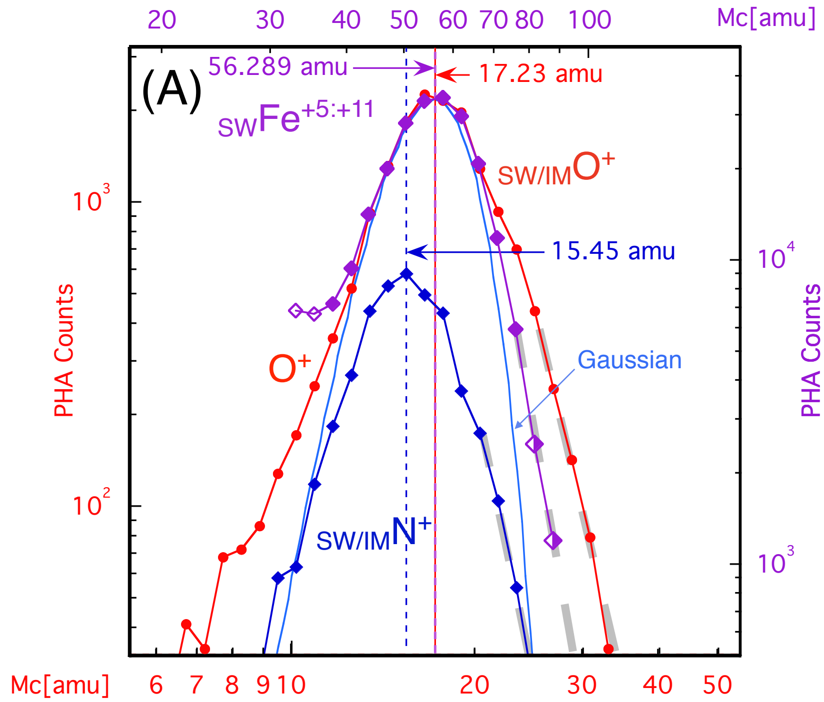

Figure S7. (A) Here we demonstrate the similarity of atomic ion mass distributions from intermediate-Mass N^+ (blue) and O^+ (red) measured in the near-Earth SW/IM plasma regime up to high-Mass high charge state, solar origin swFe ($Fe^{+5:+11}$, purple). Mc is the Mass at the center of the Mass histogram bins. The swFe is from all regimes to increase its counting statistics. O^+ and N^+ measured in the near-Earth SW/IM derives primarily from Earth's ionosphere, but both ion species are shown in Figure 9 as likely having lunar PUI flux components. No single functional form appears to fit the entire Mass distribution shapes; however, they appear to have kappa-like shapes: gaussian-like at and below the peak Mass, and power-law-like at the highest Mass values. A simple gaussian (light blue curve) and power-law lines (heavy gray lines) are shown for reference. The instruments' Mass axis values are presently uncalibrated, resulting in measured values slightly different from the ions' masses. The $swFe^{+6:+11}$ Mass_Mass-per-Charge matrix selection area is shown in Figures S7B and S7C.

swFe collection - all plasma regimes - 1995 through 2015

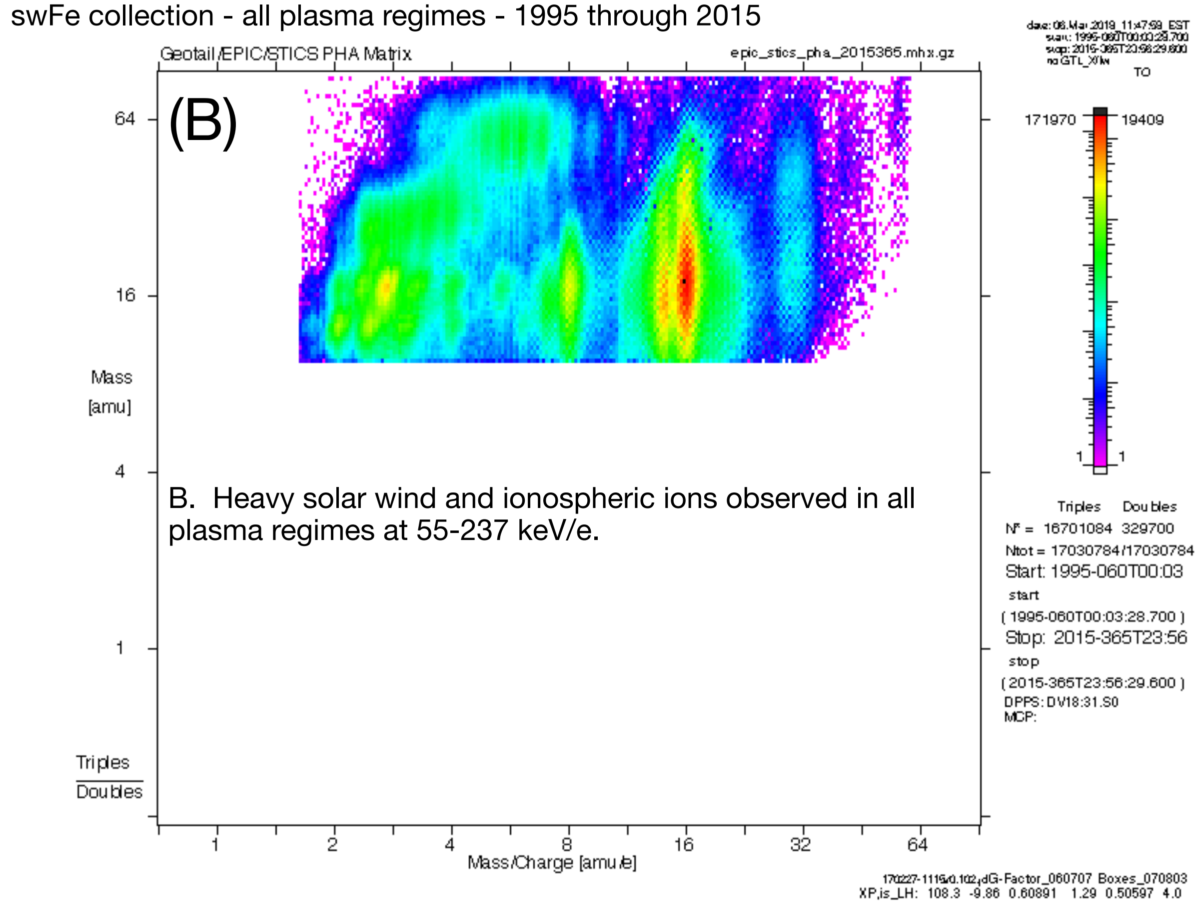

B. Heavy solar wind and ionospheric ions observed in all plasma regimes at 55-237 keV/e.

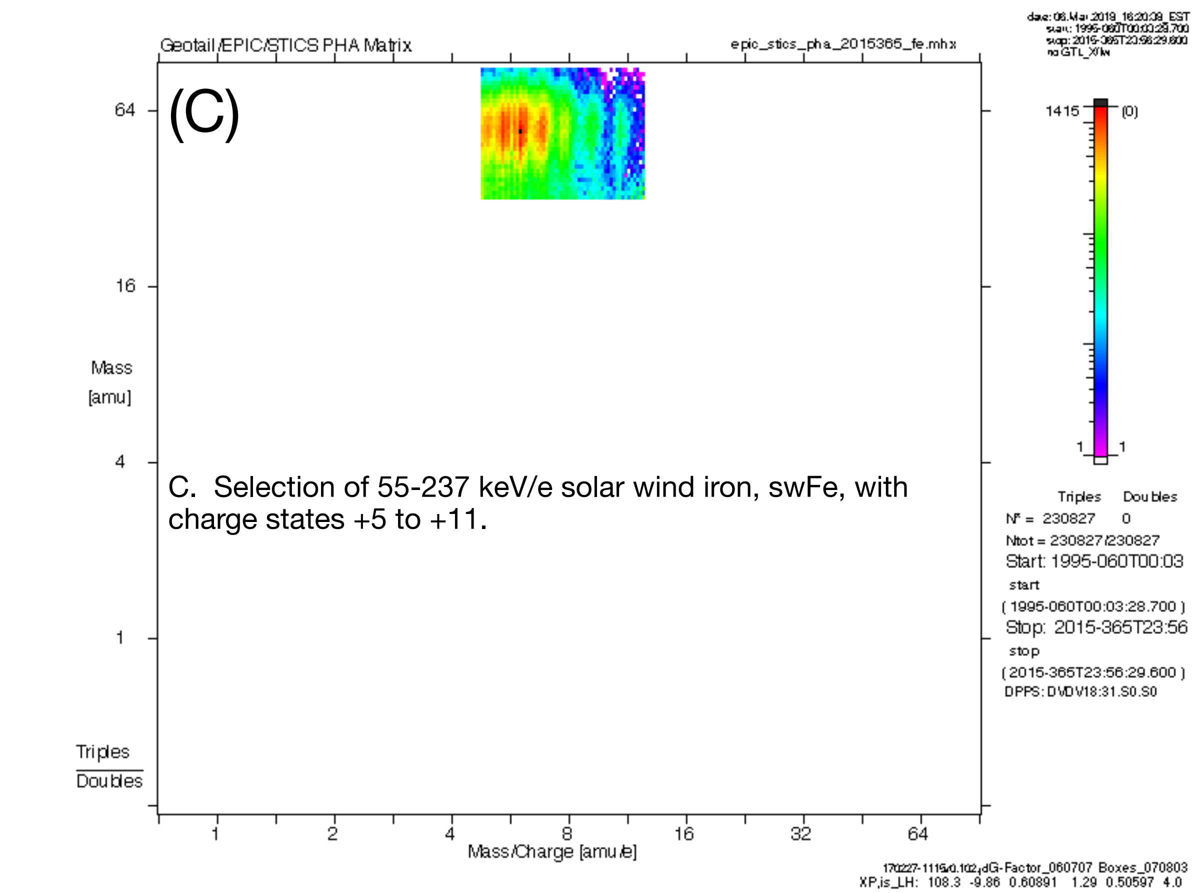

C. Selection of 55-237 keV/e solar wind iron, swFe, with charge states +5 to +11.

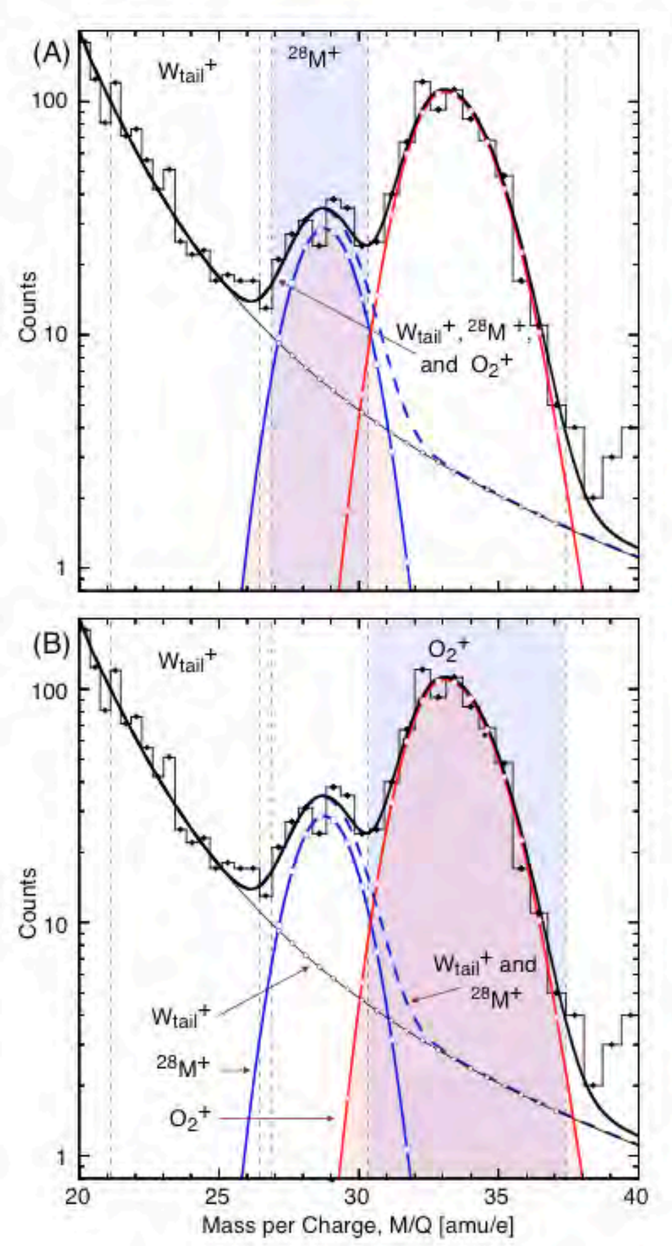

Figure S8. Specific identification of the overlap and spillover of molecular ion species curve fits for Saturn Sphere data used in Christon et al. (2013) based on laboratory calibration responses for M/Q = 28 and 32 amu/e at ~110 keV/e during Interval A. Estimates of the PHA distributions for O_2^+ and $^{28}M^+$ as well as the extended W^+ high-mass tail, which represents O^+ and three molecular constituents, OH^+, H_2O^+, and H_3O^+, are based on laboratory calibrations. (from Figure A-1 Christon et al., 2013, Supplementary Information).

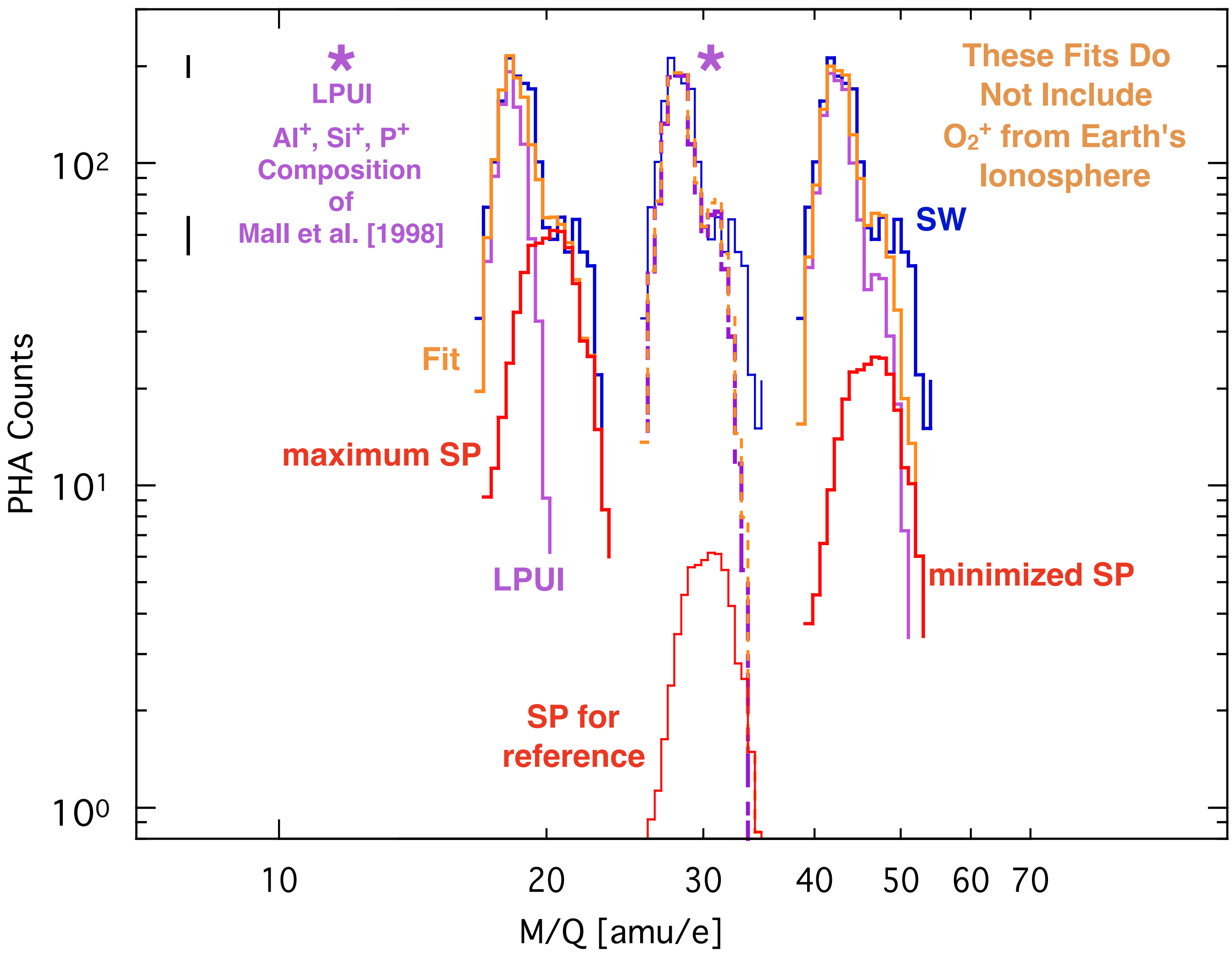

Figure S9. We demonstrate the importance of using escaped ionospheric O_2^+ to fit the SW/IM distribution <u>by leaving it out of our set of ion candidates in these fits</u>. The M/Q axis applies to the two center peaks (*LPUI and SP for reference), those to the right and left are so placed for ease of comparison. LPUI (purple) and escaped SPHERE MI (red) shapes are used to fit the SW/IM distribution (blue). On the left (right) are the maximum (minimum) SPHERE MI contributions we visually fit while maintaining the approximate shape of the SW/IM distribution within statistical uncertainty of measured counts (sample uncertainties on the far left), but not incorporating O_2^+. (middle) A fit using only the Mall et al. (1998) LPUI composition adjusted within the statistical uncertainty of their measured counts (a SPHERE MI shape is shown at very low levels for reference). In all cases the SW/IM distribution at M/Q > ~32 amu/e is not accounted for by any of these fits without using an escaped O_2^+ contribution.

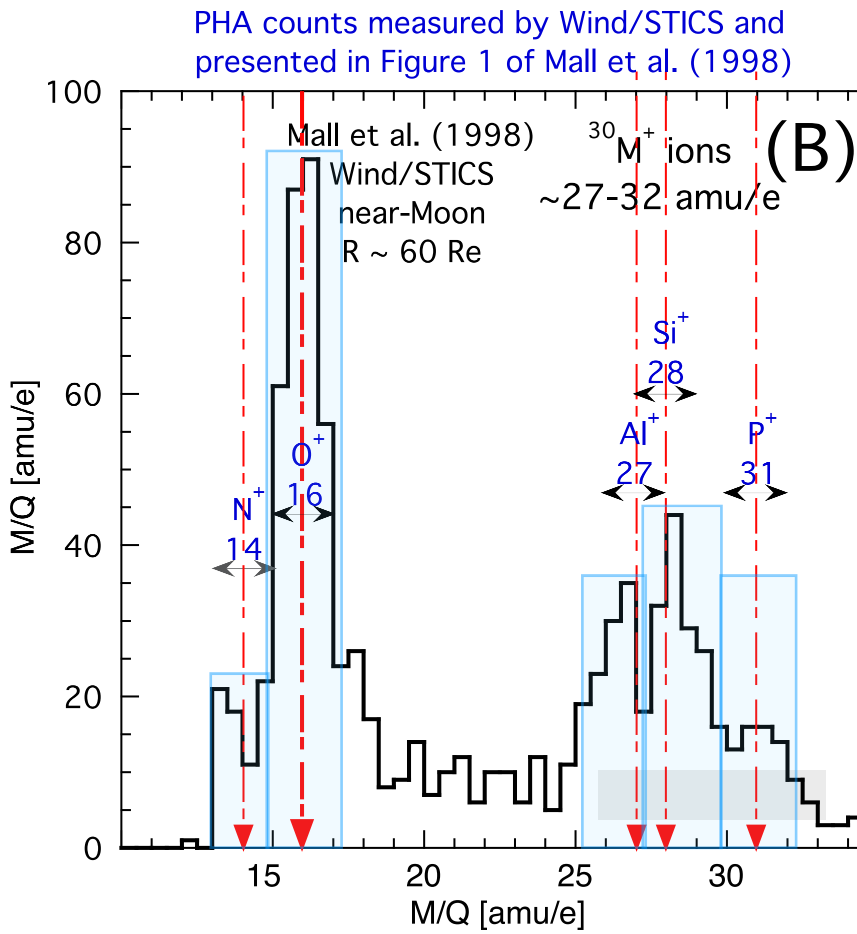

Figure S10. (A) PHA data from Figure 1 of Mall et al. (1998) which presented measurements of lunar pickup ions, PUI, including two M/Q histograms of PHA counts. The Wind/STICS ion data were obtained on the downstream (earthward) side of the Moon at >17 lunar radii when the Moon was sunward of Earth. Given the small number of PHA counts, we summed their two histograms and focus on the Mass 30 ions relevant to our study. We use only a subset of the ion species Mall et al. identified. Horizontal double headed arrows are plotted at the width of the O^+ peak. The horizontal gray-shaded section is relevant to the Mass-30 lunar PUI background addressed herein (see text). Blue boxes mark the ranges used to sum the PHA counts. The sums and ratios are:

Ions	Counts	/	Counts	-->	Ratio	±	Uncertainty
Al+ / Si+	106	/	148	Al+/Si+	0.72	±	0.09
Si+ / Si+	148	/	148	Si+/Si+	1.00	±	0.12
P+ / Si+	76	/	148	P+/Si+	0.51	±	0.07

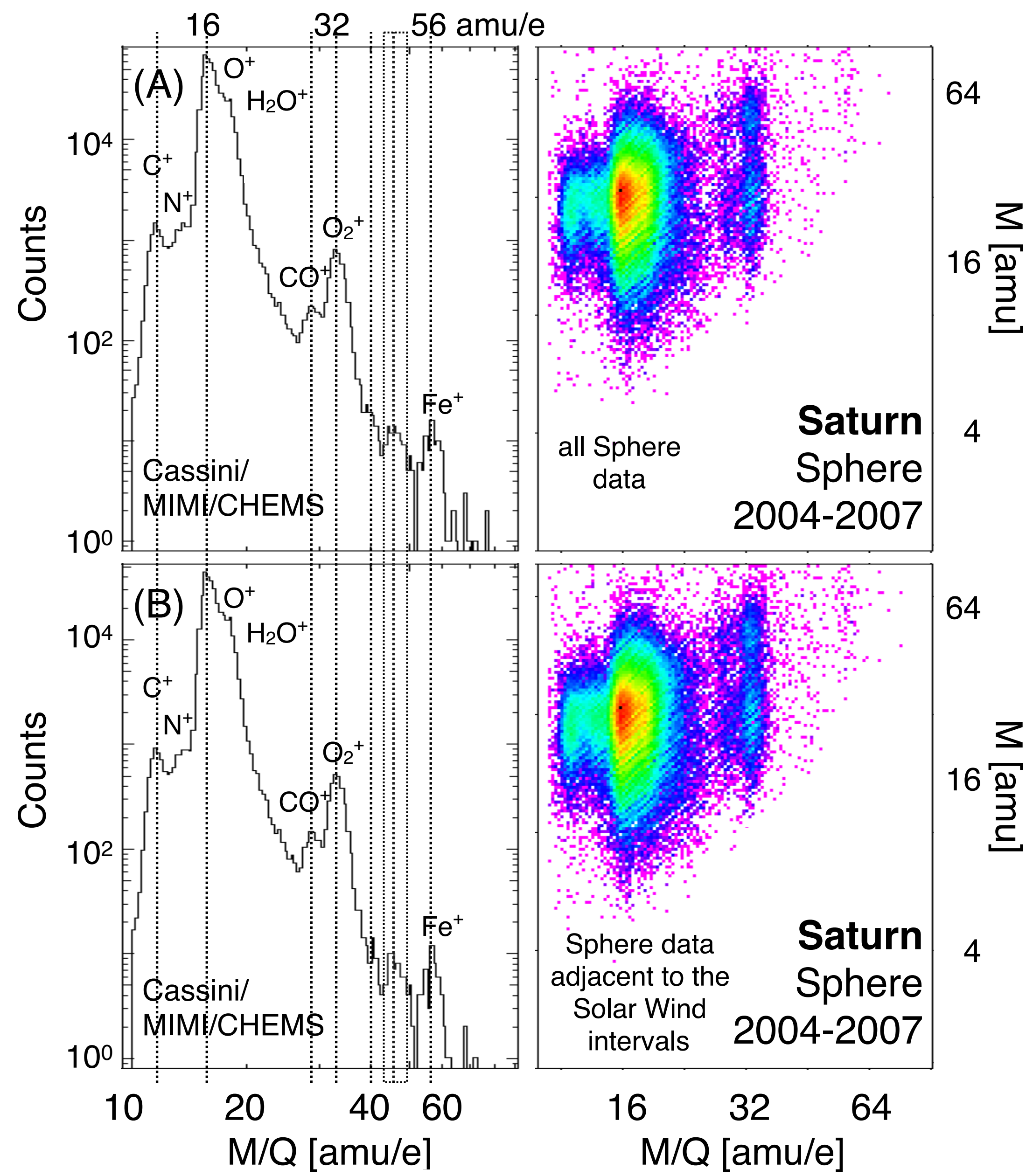

Figure S11. Cassini's measurements of Saturn's suprathermal ion populations in the SPHERE at R < 20Rs during late-2004 to mid-2007: (A, top) all intervals and (B, bottom) only SPHERE intervals before and/or after R > R_{BS} samples. Dashed lines highlight several ion peaks. Ion composition of the overall and select adjacent intervals is nearly indistinguishable.

A Scenario For Cassini's Jovian S^+ Observations

Luhmann (2003) presented in her Figures 1 and 2 a simple concept (the limited S^{+1} PUI cloud) that easily explains why Cassini/CHEMS' observed S^{+1} pickup ion PUI fluxes disappear near the start of 2002.

A breakdown of pre-Saturn Interplanetary Data, 1999 to mid-2004:
The sketched scenario below visualizes a possible explanation of the S^{+1} interplanetary measurements on Cassini's cruise to Saturn:

(1) Cassini observes S^{+1} PUIs prior to Jupiter flyby after 2000-246,
(2) at Jupiter encounter, and for a time afterward, until ~2001-110, Cassini is fully embedded in Jupiter's planetary S^{+1} PUI cloud.
(3) By ~2002-001, Jupiter's attached S^+ PUI cloud orbits past Cassini's more slowly orbitally progressing trajectory position, after which Cassini stops measuring the S^{+1}.

On the other hand, Jovian O^{+1} PUIs are much more widely distributed/dispersed (because O has a higher ionization potential than S). The jovian O^{+1} PUIs are difficult to separate from interplanetary/interstellar O^{+1} PUIs without detailed analysis.

ref: Luhmann, J. G. (2003). Expected heliospheric attributes of Jovian pickup ions from the extended neutral gas disk. *Planet. Space Sci., 51*, 387–392. https://doi.org/10.1016/S0032-0633(03)00034-5

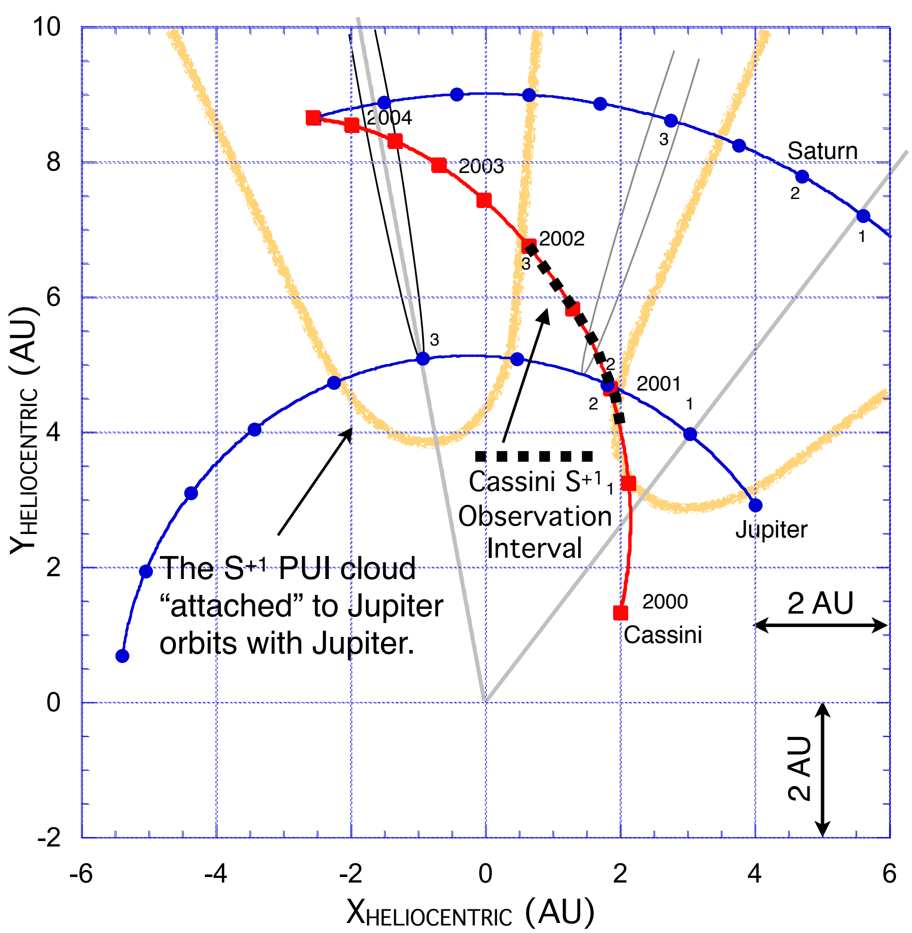

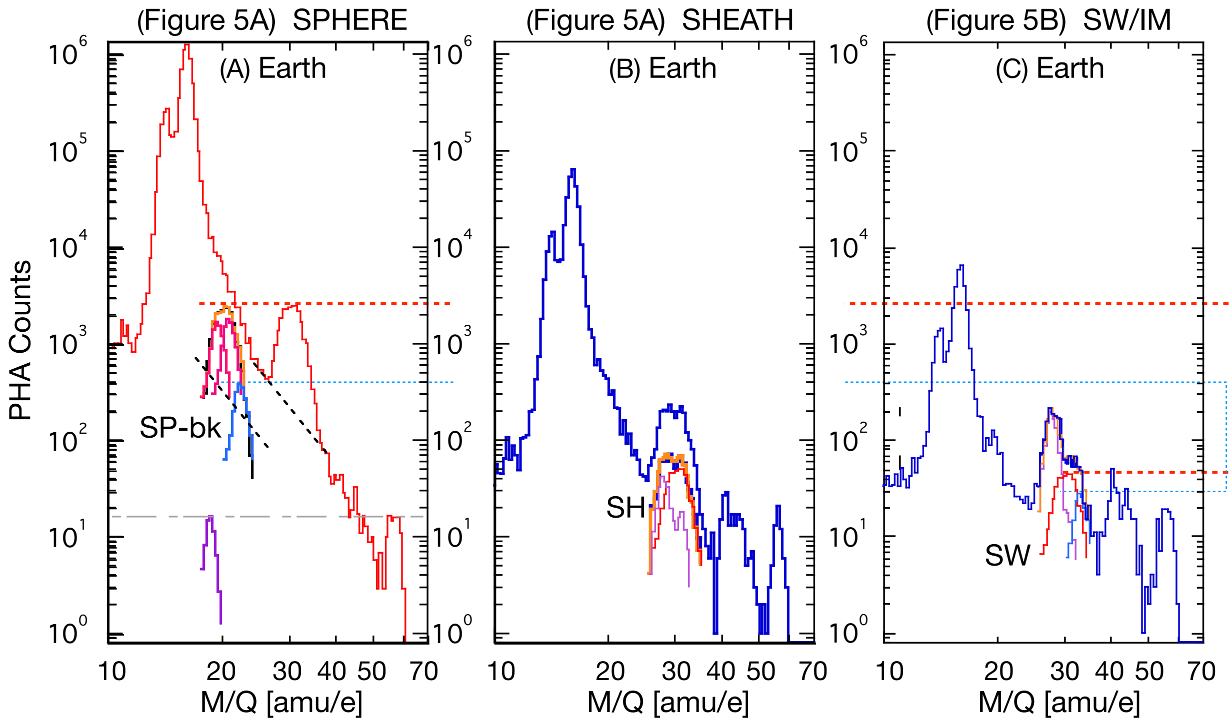

Figure S13A-C. Earth: Long-term suprathermal heavy ion composition measurements in near-Earth plasma regimes that are used in Figures 5A and 5B are plotted without being normalized to O^+ and compared directly. The vertical axes are identical. Shown are ~21 continuous years of Earth data. The Mass-30 SHEATH (B: blue) distribution is intermediate between that in the SPHERE (A, red) and SW/IM (C and D: blue). Floating insets at the bottom of the panels (see text) show very rough visual fits (orange) to the: (A) background subtracted SPHERE (SP-bk, black), (B) SHEATH (SH), and (C) SW/IM (SW) data (blue). (A) The SP-bk fit (offset horizontally for clarity) is composed of N_2^+ and NO^+ (both rose), O_2^+ (light blue), and ionospheric Si^+ (purple) distributions. (B) The SH fit (offset vertically by a factor of ~3.4) is composed of ionospheric N_2^+ and NO^+ (shown combined by the SPHERE Mass-30 shape in red) and a combination of lunar PUI, Al^+, Si^+, and P^+ (purple) distributions. (C) The SW fit (not offset), is composed of a different combination of lunar PUI (purple), the ionospheric N_2^+ and NO^+ (again shown as the SPHERE Mass-30 shape in red), and ionospheric O_2^+ (light blue). Dashed red and blue line constructs drawn across the Figure from the SW/IM to the SPHERE demonstrate that the O_2^+ peak level appears to decrease less than that of the N_2^+ and NO^+ (the red curve) as the MI escape from the SPHERE into the nearby SW/IM; which can be interpreted as suggesting that O_2^+ does not dissociate as quickly as N_2^+ and NO^+ upon reaching the solar wind plasma regime - as also appears to be the case at Saturn (see Figures S13D and S13E). Note that the O_2^+ level is constrained at approximately the level shown, whereas the N_2^+ and NO^+ can be replaced almost fully by lunar PUI (see Figure S9). See text and Figure 5.

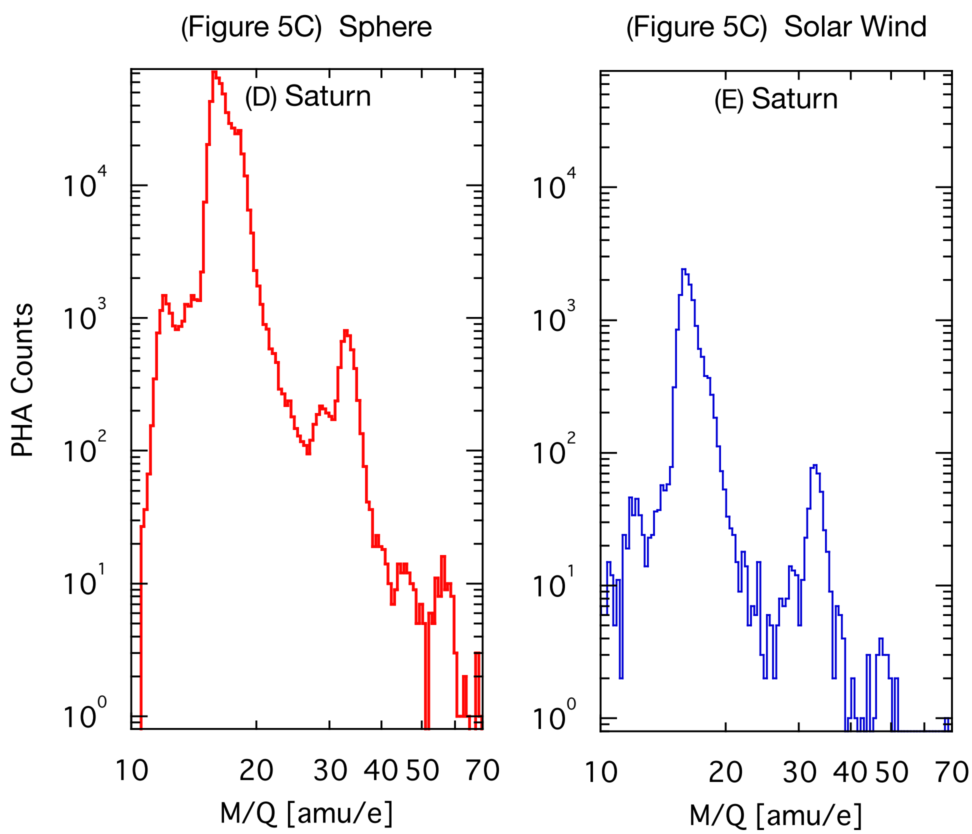

Figure S13DE. Saturn: Long-term suprathermal heavy ion composition measurements in near-Saturn plasma regimes that are used in Figure 5C are plotted without being normalized to O^+ and compared directly. The vertical axes are identical. Shown are samples from ~3 years of Saturn data; not all Solar Wind intervals at Saturn were included. The Mass-30 Sphere (D: red) distribution is reflected in the Solar Wind (E: blue). See text and Figure 5.

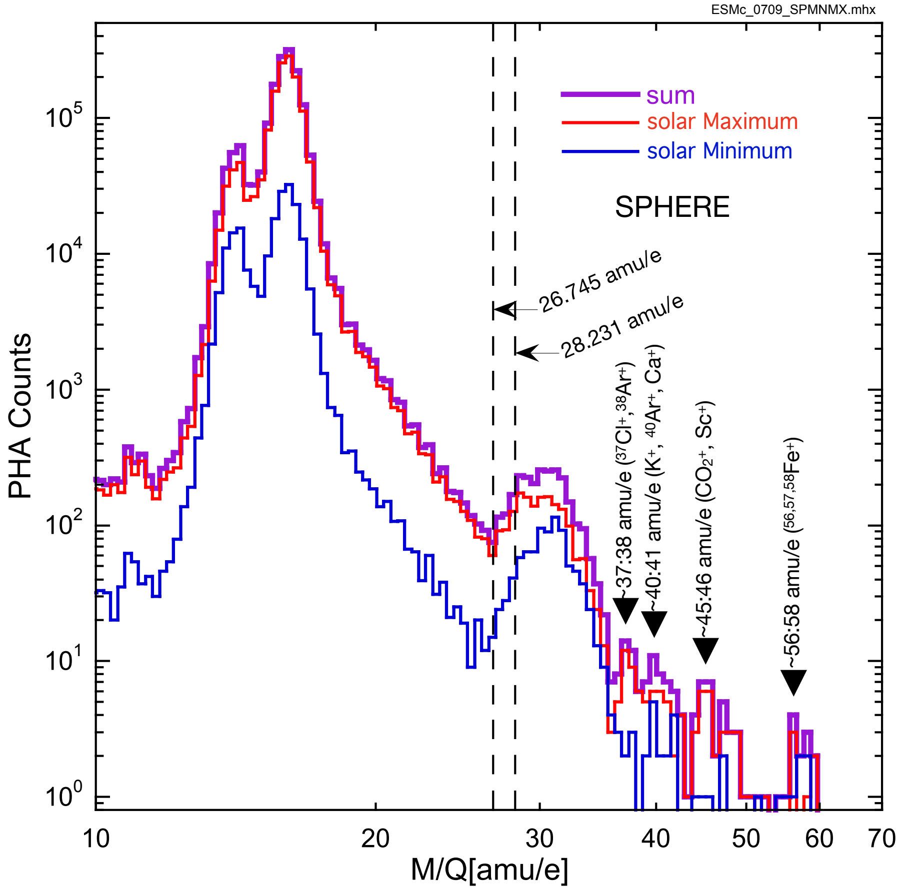

Figure S14. This Figure shows PHA data from Earth's SPHERE plasma regime from a long quiet solar minimum sample (2007, 2008, and 2009) and a moderate solar maximum sample (2000 and 2001) and their arithmetic sum. When separated into select shorter intervals chosen to highlight differences, it is apparent that some ionospheric and/or lunar Al^+ and Si^+ which may be continually present in the SPHERE likely rises to higher relative levels during solar maximum intervals. Two fiducial dashed lines drawn at 26.68 and 28.10 amu/e highlight the likely elevated Al^+ and (lower edge of) Si^+ ionospheric and/or lunar PUI distributions. This Mass-28 atomic ion signal range is probably masked in our mission-long sums because of the dominance of lower geomagnetic and solar activity conditions. At M/Q > ~35 amu/e various stable isotopes of possible metal ionospheric ion and/or lunar PUI candidate species are listed.